Available online at www.sciencedirect.com

ScienceDirect

Energy Procedia 120 (2017) 126–133

Energy Procedia

www.elsevier.com/locate/procedia

INFUB - 11th European Conference on Industrial Furnaces and Boilers, INFUB-11

Laminar Burning Velocity of Methane/Air Mixtures and Flame Propagation Speed Close to the Chamber Wall

Loreto Pizzuti [a]*, Cristiane A. Martins [a], Leila R. dos Santos [a], Danielle R. S. Guerra [b]

[a]*Technological Institute of Aeronautics, Mar Eduardo Gomes, 50, São José dos Campos – 12228-900, Brazil*
[b]*Federal University of Para, Avenida Augusto Correa, 01, Belém - 66075-110, Brazil*

Abstract

Experimental studies on the laminar burning velocity (LBV) and the flame propagation speed close to the wall of premixed methane-air flames at a pressure of 1 bar and ambient temperature, for poor and rich mixtures, have been conducted and analyzed. The methane-air mixture LBV and flame propagation speed are studied in a constant volume combustion chamber with acrylic windows using the shadowgraph technique and a high-speed camera. The recorded images are analyzed using a Matlab script and both the system and the Matlab code have been validated against literature data. The results are in quite good agreement with available literature for LBV that shows its decreasing with pressure increase. For the flame propagation speed little literature has been found for validation but using a different set-up. The results show that the flame propagation speed decreases almost linearly except close to the wall where some oscillations are present, due to a combination of multiple phenomena such as compression and heating of the unburned mixture, a combination of radiative heat loss to the wall, flame curvature and flame stretch.

Keywords: experimental laminar burning velocity; flame propagation speed close to wall; methane/air mixtures.

1. Introduction

The laminar burning velocity (LBV) is one of the most important parameters of a combustible mixture. It is a physicochemical property of the air-fuel gas mixture, and is defined as the speed at which a steady planar flame front

* Corresponding author. Tel.: +55 12 39475826;
E-mail address: loretopizzuti@gmail.com

10.1016/j.egypro.2017.07.145

propagates in a premixed, quiescent mixture in front of the flame in a direction normal to the plane [1, 2]. The LBV is a unique value of flame speed for a gas of a fixed composition, initial temperature and pressure, without further specification of hydrodynamic conditions, such as stretch rate, Reynolds number, etc [3, 4]. On a practical level, the LBV affects the fuel burning rate in internal combustion engines (ICEs) and the engine's performance and emissions. On a fundamental level, the burning velocity is an important target for kinetic mechanism development and validation. Accurate determination of laminar burning velocity is extremely important for the development and validation of kinetic mechanisms for gasoline, diesel surrogate fuels and alternative fuels [5].

Knowledge of flame propagation close to a wall and flame –wall interactions are of increasing importance as those concepts are related to relevant engineering applications such as possible misfiring in ICEs, optimization of combustion, and reduction of unburned hydrocarbons in the combustion products [6]. Most of the experimental studies on the flame –wall interaction have been done on thin channels [6, 7] or over rotating vessels [8, 9].

In the present article, we present the results of a laminar burning velocity study and flame propagation speed close to the wall in a cylindrical constant volume combustion chamber (CVCC). Methane-air premixed flames at ambient temperature and initial pressure of 1 bar and equivalence ratios between 0.58 and 1.43 are taken into account. The laminar burning velocity is compared with values present in the literature while the flame propagation speed data close to the wall are presented as new data because no results have been found in the literature for such a configuration. However, the image processing allows the determination of the flame radius up to a minimum distance from the wall of approximately 2.5 mm.

2. Experimental Set-up

The experiments are performed in a cylindrical CVCC with three acrylic windows for optical access. The chamber is made of 304 stainless still and its internal diameter and length are 150 mm (that allow the visualization) and 170 mm, respectively. Figure 1 shows the most relevant measures in a 3D vision of the CVCC with the chamber core and the flanges to fix the optical windows.

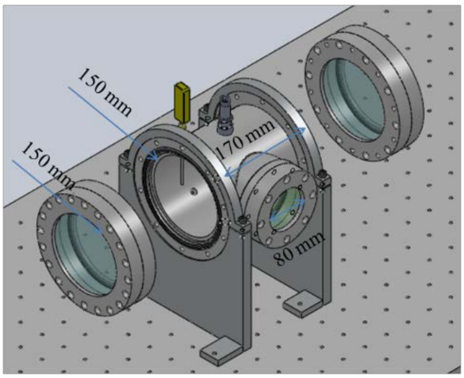

Fig. 1. 3D view of the CVCC with measures.

A k-type thermocouple is used to measure the initial temperature in the chamber, while a Kistler 701A piezoelectric pressure transducer, with a Kistler 5018A charge amplifier is used to record the pressure evolution inside the chamber. A couple of automotive spark plugs, modified with extended tungsten electrodes, are used to get the ignition at the center of the CVCC. The mixtures are made of certified 99.5 % purity methane and compressed air. The mixtures are prepared in an auxiliary cylinder of 20 liters by using the partial pressure technique and a gas chromatography is used to check the composition. Therefore, the CVCC is filled with the mixture at the desired pressure and after five minutes of rest is ignited. An absolute pressure transducer with the measuring range between 0-12 bar is installed in the filling line allowing to use the partial pressure technique. A safety valve is installed along the filling line close to the CVCC and it is set to open at 39 bar, which is the pressure safety limit of the optical windows. A vacuum pump with a nominal vacuum of 10 mbar is responsible for the vacuum in the CVCC and the filling line.

The shadowgraph technique is used to record the flame evolution images from which the LBV and the flame propagation speed close to the wall are determined by using an image processing program. Figure 2 shows a sketch of the shadowgraph arrangement used in this experiment. The shadowgraph technique allows the visualization of the second derivative of density variation in the test section. A PCO Dimax S1 high-speed camera allows to record up to 4000 fps at full resolution (1008x1008 pixels).

A self-written LabVIEW program controls the trigger and the experiments acquisition data by using a National Instruments USB 6259 board. The program controls the high-speed camera, the piezoelectric pressure transducer, the ignition system and the thermocouple. The program allows controlling the trigger signal for the spark ignition module and the recording of data from the other equipment. The flame images of the high-speed camera are processed by using a program written in Matlab, based on the work of Buffel and Bauwens [2], released for free utilization. However, some modifications have been done due to the different CVCC configuration.

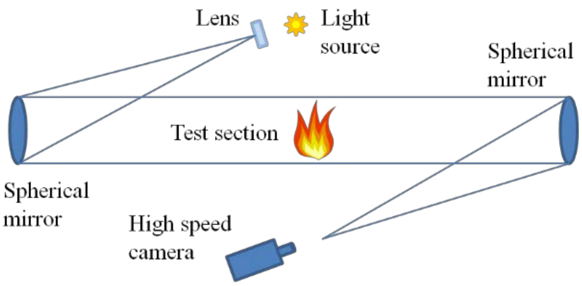

Fig. 2. Sketch of the shadowgraph technique.

3. Equations

The LBV is determined using the optical technique. In this technique, the hypothesis of no influence from natural convection on a propagating spherical flame is assumed. It means that, the unburned gas is isotropic and maintains its initial temperature, the burned gases do not diffuse and the pressure equalizes inside the reactor. The outwardly flame propagation is recorded using the shadowgraph technique and a high-speed camera. These images are used to determine the flame propagation speed, S_b, according to eq. (1), r_b is the flame radius determined from the images:

$$S_b = \frac{dr_b}{dt} \tag{1}$$

In real applications, it is impossible to generate adiabatic, planar, one-dimensional flames so that the flame front is always subjected to stretch effects. The flame response to stretch has been studied by many researchers [10, 11], by considering the Markstein length of the burned gases, L_b, which expresses the dependence of flame velocity on stretch [12]:

$$S_b^0 - S_b = L_b\, \kappa \tag{2}$$

Where S_b^0 is the unstretched flame propagation speed of the burned mixture and S_b is given by equation (1). The stretch rate κ is defined in each point of the flame surface as [13]:

$$\kappa = \frac{1}{A}\frac{dA}{dt} \tag{3}$$

A is the flame front surface. For a spherical flame, the stretch rate is given by the equation (4):

$$\kappa = \frac{1}{r_b}\frac{dr_b}{dt} = \frac{S_b}{r_b} \tag{4}$$

The spherical flame is a positively stretched flame due to its surface increase with time. In this method S_b^0 is determined by linear extrapolation from the $S_b - \kappa$ graph, for $\kappa = 0$. The Markstein length, L_b, is determined from equation (2). The unstretched laminar burning velocity, S_u^0, is determined to apply the continuity law to a planar unstretched flame, ρ_b and ρ_u are the burned and unburned gas densities, respectively.

$$S_u^0 = S_b^0 \frac{\rho_b}{\rho_u} \tag{5}$$

4. Analysis and Results

In this section the experimental results will be presented and analyzed. The LBV results and the flame propagation speed close to the wall are presented in separate subsections.

4.1. Laminar burning velocity

The results for LBV are obtained for the initial pressure of 1 to 2 bars inside the CVCC. There is a large literature on LBV of methane-air mixtures at atmospheric pressure. Figure 3 shows a comparison of the LBV determined in this work, as the mean of three experiments data with the most relevant literature, showing a quite good agreement. The horizontal error bar refers to the uncertainty in the mixture composition due to the partial pressure method considering preparing 2.5 bars of CH_4/air mixture in the auxiliary cylinder for each equivalence ratio. The vertical error bar refers to the overall statistical uncertainty in S_u^0 calculation, which is within 11 % for this system. The combined uncertainty on initial temperature, pressure and composition is within ± 6 % close to stoichiometry, and within ± 9 % close to flammability limits. The combined confinement and radiation effect is within 3.6 % for $0.7 \leq \phi \leq 1.3$ and within 6.5 % for equivalence ratio close to flammability limits, whereas uncertainties due to linear stretch behavior is within 2 %. The combined confinement and radiation effect always brings to a reduction in S_u^0 determination whereas linear stretch behavior always introduces an overestimation of S_u^0. The overall statistical uncertainty in S_u^0 is obtained considering all the individual groups of uncertainties.

Figure 4 presents a comparison between experimentally determined LBV at initial pressures of 1 and 2 bars respectively. As expected, the LBV decreases with increasing of the initial pressure.

4.2. Flame propagation speed close to the wall

The flame propagation speed close to the wall has been determined up to a distance of approximately 2.5 mm from the wall due to the limitation of the image processing. The flame propagation speed is given as a function of the flame radius in the following figures. Figure 5 shows S_b versus flame radius for three experiments at an equivalence ratio of 1.07 and 1.43, respectively, showing quite a good repeatability.

Figure 6 shows the flame propagation speed behavior for different equivalence ratio mixtures, from $\phi = 0.77$ to $\phi = 1.43$ plotting the results of the first experiment for each mixture. For equivalence ratio of the mixture close to stoichiometry the flame propagation speed is the highest when considering a region distant from the wall. Moreover, while getting closer to the wall the behavior of the flames is similar, decreasing almost linearly up to a radius of approximately 62 mm.

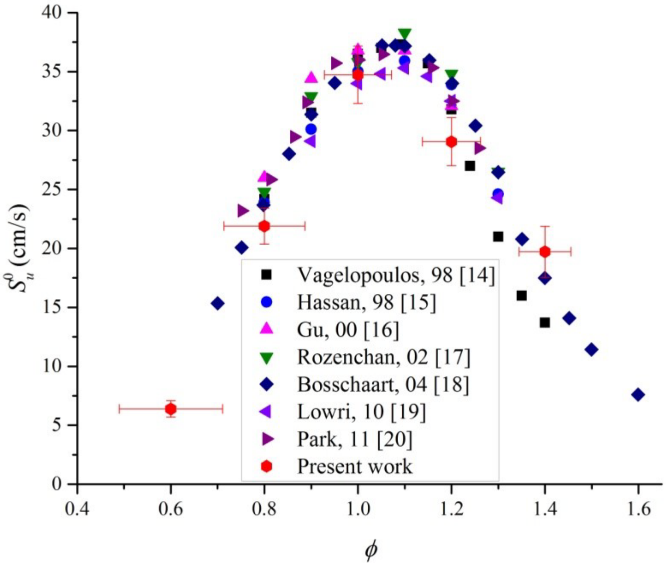

Fig. 3. Comparison of LBV values from literature with present work results, in red hexagons, for methane – air mixtures at initial pressure of 1 bar and ambient temperature, 25º C.

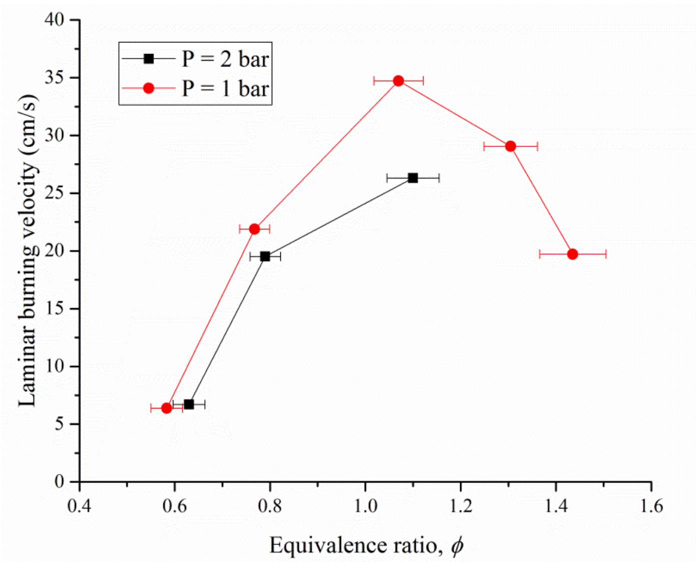

Fig. 4. LBV of methane - air mixtures at an initial pressure of 1 and 2 bars and ambient temperature, 25º C.

Figure 6 shows the flame propagation speed behavior for different equivalence ratio mixtures, from ϕ = 0.77 to ϕ = 1.43 plotting the results of the first experiment for each mixture. For equivalence ratio of the mixture close to stoichiometry the flame propagation speed is the highest when considering a region distant from the wall. Moreover, while getting closer to the wall the behavior of the flames is similar, decreasing almost linearly up to a radius of approximately 62 mm.

However, as clearly shown in Figure 7, which presents a zoom closer to the wall region, when getting closer to the wall, the flame propagation speed, instead of decreasing exponentially to zero as expected from the simulation presented in Figure 8, presents oscillations.

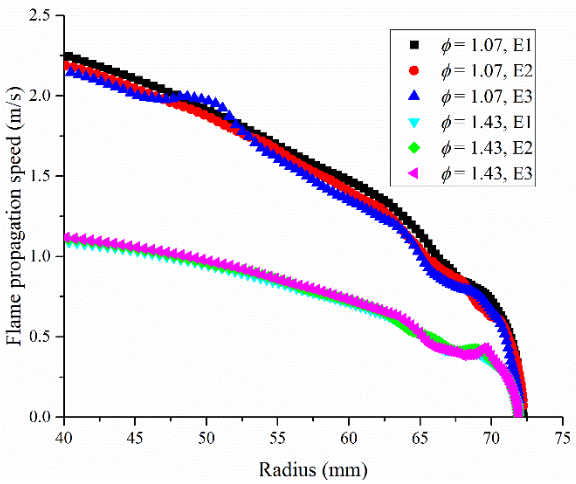

Fig. 5. Flame propagation speed behavior for CH_4-air mixtures at ambient temperature and P = 1 bar, for ϕ = 1.07 and ϕ = 1.43.

Multiple phenomena should be taken into account when analyzing the flame propagation speed close to the wall. The unburned mixture is compressed and heated, thus changing the mixture reaction rate. In addition, a combination of flame/wall interaction, radiative heat loss to the wall, flame curvature and flame stretch should be considered [21]. The oscillations in the flame propagation speed of Figures 6 and 7, that start at approximately 10 mm from the cylinder wall, results from the combination of the phenomena mentioned before. The impact of low-temperature combustion for lean mixtures on wall heat flux induced by temperature differences between the preheated temperature of the fuel mixture and the wall has found to be insignificant by Yenerdag et al. [22].

An additional phenomenon that occurs when the pressure of the residual mixture increases is the cellular flame. This phenomenon leads to the break of the flame surface in large cells which increase the flame surface and increase the flame propagation speed. The combination of different instability mechanisms is responsible for the appearance of cellular flames in premixed flames. The most important are hydrodynamic, based on the Darrieus and Landau theory, and the diffusional-thermal mechanisms [23].

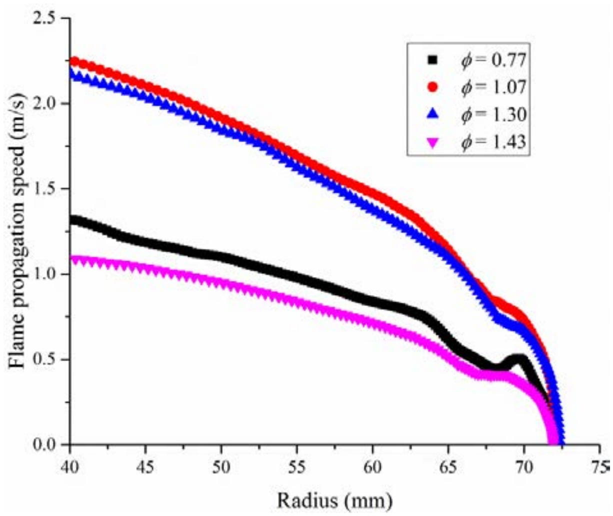

Fig. 6. Flame propagation speed behavior for CH_4-air mixtures at ambient temperature and P = 1 bar.

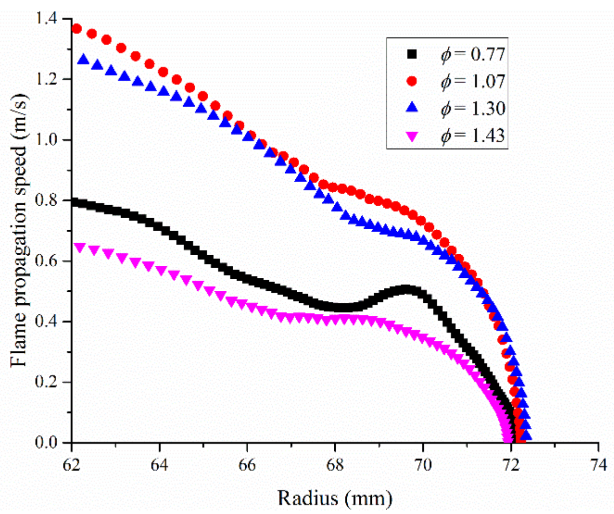

Fig. 7. Zoom in the region close to the wall

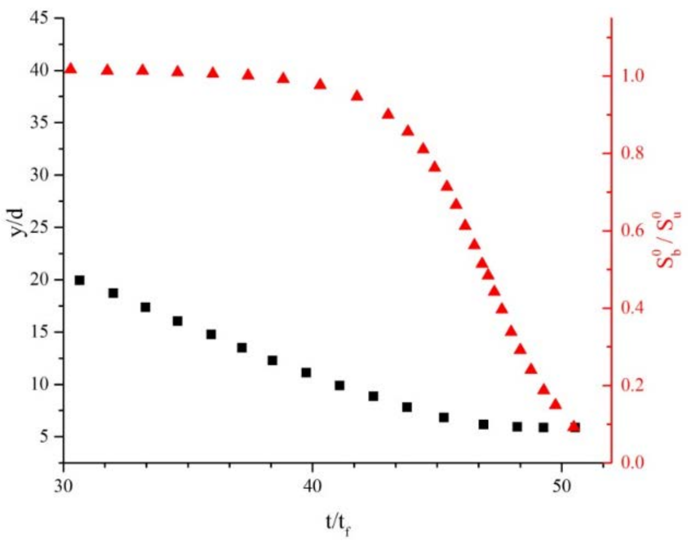

Fig. 8. Time evolution of normalized flame / wall distance y/d and flame propagation speed for a stoichiometric premixed flame. In this figure y is the distance from the wall and d is the flame thickness. Adapted from Lataillade et al. [24].

The image processing, used for flame propagation speed calculation, may give less accurate results when applied to cellular flames because the flame surface becomes corrugated but the technique still determines an ideal spherical flame for determining the flame radius.

Figures 9a and 9b show two images of the flame surface taken with the high-speed camera. In the first image the flame surface is stable while in the second the flame surface is starting to be affected by cellularity.

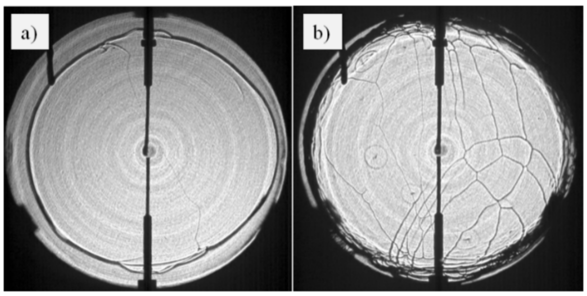

Fig. 9 a) Stable flame surface. b) Cellular flame.

5. Conclusions

In this study, the experimentally determined laminar burning velocity and flame propagation speed close to the wall of laminar premixed methane-air flames have been presented. Mixtures with equivalence ratio from 0.58 to 1.43 at ambient temperature and initial pressure of 1 bar have been analyzed. The most relevant conclusions are the following: The laminar burning velocity is in quite good agreement with the literature, which validates the experimental set-up and the sequence of data processing. The laminar burning velocity decreases when increasing the initial pressure. The flame propagation speed decreases almost linearly to zero except close to the wall were some oscillations are present due to the combination of multiple phenomena, i.e., compression and heating of the unburned mixture, a combination of radiative heat loss to the wall, flame curvature and flame stretch.

Suggestion for future works is to study mixtures with higher initial pressure in order to verify the influence of cellular flame on flame propagation speed close to the wall. Moreover, the heat transfer to the wall should be quantified in order to relate the flame propagation speed with the flame heat transfer.

Acknowledgement

The authors are grateful to FAPESP (Fundação de Amparo à Pesquisa do Estado de São Paulo) for the support of this work through project 2010/51315-3.

References

[1] Law CK. Combustion Physics. New York: Cambridge University Press. 2006
[2] Buffel L, Bauwens J. Laminar burning velocity measurements using the GUCCI setup. Msc Dissertation. Ghent University, 2014
[3] Huzayyin AS, Moneib HA, Shehatta MS, Attia AMA. Laminar burning velocity and explosion index of LPG-air and propane-air mixtures. Fuel 2008;87:39-57.
[4] Burke MP, Qin X, Ju Y, Dryer, FL. Measurements of hydrogen syngas flame speeds at elevated pressures, Proc 5th US Comb Meet, San Diego, CA, United States, 2007
[5] Chen Z, Burke MP, Ju Y. Effects of Lewis number and ignition energy on the determination of laminar flame speed using propagating spherical flames. Proc Combust Inst 2009;32:1253-60.
[6] Gutkowski A, Tecce L, Jarosiǹski J. Flame quenching by the wall–fundamental characteristics. J KONES, 2007;14:3
[7] Daou J, Matalon M. Influence of conductive heat-losses on the propagation of premixed flames in channels. Combust Flame 2002;128: 321–39
[8] Jarosiǹski J, Gorczakowski A. The mechanism of laminar flame quenching under the action of centrifugal forces. Combust Sci Technol 2006;178:1441–56.
[9] Jarosiǹski J, Veyssiere B. Combustion phenomena: selected mechanisms of flame formation, propagation, and extinction. CRC Press. 2009
[10] Clavin P, Williams FA. Effects of molecular diffusion and of thermal expansion on the structure and dynamics of premixed flames in turbulent flows of large scale and low intensity. J Fluid Mech 1982;116: 251-82
[11] Matalon M, Matkowsky BJ. Flames as gasdynamic discontinuities. J Fluid Mech 1982;124:239-59.
[12] Giannakopoulos GK., Gatzoulisa A., Frouzakisc CE, Matalon M., Tomboulides AG. Consistent definitions of "Flame Displacement Speed" and "Markstein Length" for premixed flame propagation. Combust Flame 2015;162:1249-64.
[13] Williams FA. Combustion Theory. 2nd. ed Westview Press, 1985
[14] Vagelopoulos CM, Egolfopoulos FN. Direct experimental determination of laminar flame speeds. Proc Combust Inst 1998;27: 513–19
[15] Hassa MI, Aung KT, Faeth GM. Measured and predicted properties of laminar premixed methane/air flames at various pressures. Combust Flame 1998;115: 539–50.
[16] Gu XJ, Haq MZ, Lawes M, Woolley R. Laminar burning velocity and Markstein lengths of methane-air mixtures. Combust Flame 2000;121:41-58.
[17] Rozenchan G, Zhu DL, Law CK, Tse SD. Outward propagation, burning velocities, and chemical effects of methane flames up to 60 atm. Proc Combust Inst 2002;29:1461–69.
[18] Bosschaart KJ, De Goey LPH. The laminar burning velocity of flames propagating in mixtures of hydrocarbons and air measured with the heat flux method. Combust Flame. 2004;136:261–9.
[19] Lowry W, De Vries J, Krejci M, Petersen EL. Serinyel Z, Metcalfe W, Curran H, Bourque G. Laminar flame speeds measurements and modeling of pre alkanes and alkane blends at elevated pressures. J. Eng Gas Turbines Power. 2010;133:019102.
[20] Park O, Veloo PS, Liu N, Egolfopoulos FN. Combustion characteristics of alternative gaseous fuels. Proc Combust Inst 2011;33: 887–94.
[21] Chen Z, Ju Y. Theoretical analysis of the evolution from ignition kernel to flame ball and planar flame. Combust Theory Modell 2007;11: 427–53.
[22] Yenerdag B, Minamoto Y, Aoki K, Shimura M, Nada Y, Tanahashi M. Flame–wall interactions of lean premixed flames under elevated, rising pressure conditions. Fuel; 2017;189:8–14.
[23] Kwon OC, Rozenchan G, Law CK. Cellular instabilities and self-acceleration of outwardly propagating spherical flames. Proc Combust Inst 2002;29:1775–83.
[24] Lataillade A, Dabireau F, Cuenot B, Poinsot T. Flame / wall interaction and maximum wall heat fluxes in diffusion burners. Proc Combust Inst 2002;29:775–9.